IJCRT.ORG ISSN: 2320-2882



INTERNATIONAL JOURNAL OF CREATIVE RESEARCH THOUGHTS (IJCRT)

An International Open Access, Peer-reviewed, Refereed Journal

"Harnessing Ternary Metal Oxide Synergy: Electrochemical Design Of Zno/Zro₂/Al₂O₃ Nanocomposite For Advanced Photocatalytic And **Antibacterial Applications**"

Vivekraj Nagaraju¹, Jagadish Krishnegowda², Prakash Gavisiddegowda², Umashankara Muddegowda³, Kumara Manikyanahally Narasigowda^{1,*}

- 1. Department of Chemistry, Yuvaraja's College, University of Mysore, Mysuru, Karnataka state, 570005, India.
- 2. Department of Chemistry (PG), Sarada Vilas College, University of Mysore, Mysuru Karnataka state, 570006, India.
- 3. Department of Studies in Chemistry, Karnataka State Open University, Mukthagangothri, Mysuru, and Karnataka state, 570006, India.

Abstract: A highly efficient ZnO/ZrO₂/Al₂O₃ ternary nanocomposite was synthesized using a green and cost-effective electrochemical method. The crystallinity, morphology, elemental composition, surface adsorption (BET), optical, catalytic and biological properties of the nanocomposite was systematically characterized using advanced analytical techniques. XRD analysis confirmed the presence of distinct peaks corresponding to ZnO, ZrO₂ and Al₂O₃ indicating the successful formation of a visible-light-active catalyst. SEM images revealed strong interfacial interactions between ZnO and ZrO₂ integrated within the porous, high-surface-area structure of Al₂O₃, UV-DRS analysis determined the band gap energy to be 2.75 eV. The nanocomposite demonstrated excellent photocatalytic efficiency in degrading Indigo Carmine (IC) dye, achieving up to 95% removal. The high surface area of Al₂O₃ (185 m²/g) facilitated dye adsorption, while the ZnO-ZrO₂ heterojunction enhanced charge separation: UV light-excited electrons from ZnO were transferred to ZrO₂ reducing recombination. Additionally, the nanocomposite exhibited significant antimicrobial activity against various bacterial and fungal strains, outperforming standard references. These findings highlight the potential of ZnO/ZrO₂/Al₂O₃ as an effective photocatalyst for the treatment of dyecontaminated industrial wastewater.

I. Introduction

In nanotechnology, matter with at least one dimension between 1 and 100 nanometers (nm) is manipulated[1-3]. At this size, which is referred to as the nanoscale, surface area and quantum mechanical phenomena significant role in characterizing characteristics of matter[4-5]. This concept of nanotechnology encompasses all forms technology and study pertaining to these unique characteristics [6-8]. Research and applications

that share the characteristic of scale are frequently referred to as "nanotechnologies" or "nanoscale technologies" in the plural [9-10]. Surface science, organic chemistry, molecular biology, semiconductor physics, energy storage, engineering, microfabrication and molecular engineering are among the scientific disciplines the broad definition of under nanotechnology[11-13]. From molecular selfassembly to extensions of traditional device physics, the related research and applications cover anything from creating new materials with nanoscale dimensions to controlling matter directly at the atomic level[14-15].

Because of the huge surface area of the reinforcement, even a little amount of nanoscale reinforcement can have a noticeable impact on the composite's macroscale characteristics[16-18]. instance, the electrical and thermal conductivity is enhanced by the addition of carbon nanotubes[19-20]. Other types of nanoparticulates can lead to improved mechanical strength, stiffness and resistance to wear and damage as well as improved optical, dielectric and heat resistant qualities [21]. Asymmetric nanoparticle orientation and arrangement, interface density per unit volume of the nanocomposite, thermal mismatch at the interface, nanoparticle polydispersity all have a substantial impact on the effective thermal conductivity of nanocomposites [22-25].

Modern optoelectronic devices require metal oxides because of their special optical and electrical characteristics [26-27]. Because metal oxides are semiconductors and can identify reducing and oxidizing species, they are ideal for gas sensing[28-29]. A useful family of materials for technological advancement, metal oxides have a wide range of applications in gas sensing, optoelectronics, biomedicine. energy, environmental remediation and catalysis[30-31]. Metal oxides' varied qualities and capacity to be customized for certain purposes make them essential materials with a broad range of uses [32]. Among many other areas, they are essential for energy storage, environmental cleanup, and catalysis [33-35]. They are adaptable for a range of applications since their structure, morphology and composition greatly influence their properties, which include optical, electrical and catalytic qualities[36].

Metal oxides essential are to nanocomposites because they improve their characteristics and increase their range of uses[37]. They are useful in fields including energy storage, sensing and environmental cleanup because they enhance surface area, stability and catalytic activity[38-39]. In this work, the characteristics and possible applications of metal oxide nanoparticles and nanocomposites based on TiO₂, ZnO, SnO₂, ZrO₂, Fe₃O₄, CuO and Al₂O₃ for environmental applications examined[40-41] . The article examines the crystallochemical structures of several metal oxides, their surface structure characteristics, and potential surface phenomena in air and water environments [42-43]. To help with more effective use, their physical, chemical, sorptive and photocatalytic characteristics are also given [44].

2. Materials and methodology

2.1. Materials

Alfa Asear provided the zirconia, zinc and aluminum metal wires, Alfa Asear provided the sodium bicarbonate and Elico Pvt Ltd provided the platinum electrode. Deionized water from the PURELAB extreme water purification system was utilized in each experiment. All compounds were utilized precisely as given and no further purification took place.

2.2. Methodology

2.2.1. Electrochemical synthesis of ZnO/ZrO₂/Al₂O₃ nanocomposite

ZnO/ZrO₂/Al₂O₃ nanocomposites electrochemically synthesized using copper, zirconia, and aluminum wires. The synthesis was carried out using an alkaline solution, a platinum electrode, and 0.5% NaHCO₃ as a conducting salt. The electrodes are surrounded by electrolytic solution and positioned in a holder with a 1 cm space between them. For six hours, 30 milliliters of NaHCO₃ were electrolyzed at temperature without stirring. The potential has been adjusted to raise the current to 20 mA. During the electrolysis process, zirconia, copper and aluminum electrodes act as anodes and start to dissolve, releasing Zr⁴⁺, Zn²⁺ and Al³⁺ ions. The ZnO/ZrO₂/Al₂O₃ nanocomposite is then created by electrochemically combining these ions with sodium bicarbonate solution. Because of their different redox potentials, Zr⁴⁺, Zn²⁺ and Al³⁺ions undergo electrochemical reactions at different rates. ZrO₂ and ZnO form more slowly than Al₂O₃ due to the fact that zirconium dissolving potential (-1.53 eV) is more negative than those of zinc (-0.76 eV) and aluminum (-1.66 eV). The produced nanocomposite is centrifuged and calcined for two hours at 700 °C to eliminate all of the sodium and hydroxide impurities that were produced during the electrolysis, after a continuous washing with distilled water to eliminate all of the sodium bicarbonate. The electrochemical synthesis of ZnO/ZrO₂/Al₂O₃ is explained by the mechanism below.

2.2.2. Photodegradation of IC dye using ZnO/ZrO₂/Al₂O₃ under UV light

A solution of Indigo Carmine (IC) dye with a specific concentration (0.0 ppm to 50 ppm) in de-ionized water was prepared in order to study photodegradation of IC dve ZnO/ZrO₂/Al₂O₃ under sunshine. By mixing a predetermined amount of ZnO/ZrO₂/Al₂O₃ nanocomposite catalyst in the dye solution and agitating it for 15 to 30 minutes in the dark, adsorption-desorption equilibrium was achieved. After that, the solution is constantly agitated in a photocatalytic reactor while it is exposed to UV light. Aliquots of the solution are periodically removed to observe dye degradation. The catalyst is then removed by centrifugation and the solution is then measured at 610 nm using a UV-Vis spectrophotometer. Optimization experiments can be performed by varying the starting dye concentration, pH, catalyst dosage, and irradiation time. The catalyst reusability can also be confirmed by retrieving, cleaning and reusing it in later deterioration cycles.

2.2.3 Biological activity

2.2.3.1. Anti-bacterial activity

A few Gram-positive and Gram-negative microorganisms were tested against the generated ZnO/ZrO₂/Al₂O₃ to determine their antibacterial efficacy. Gram-negative bacterial strains such Pseudomonas aeruginosa (ATCC10145) and Gram-positive strains like Listeria monocytogenes (ATCC 13593), Staphylococcus aureus (ATCC 700699) and Bacillus subtilis (ATCC 21332) were included in this investigation. A normal inoculum suspension containing 106 bacterial colonyforming units was used. Each synthesized ZnO/ZrO₂/Al₂O₃ (1 mg/mL) was prepared as a separate stock solution in dimethylsulfoxide (DMSO, v/v). The well diffusion method was used to examine the bacterial activity. The generated bacterial inoculums were evenly dispersed on a Muller-Hinton agar plate using a sterile L-shaped glass rod. Following the preparation of the wells (9 mm in diameter) using a sterile cork borer, 100 μL of the test composite was applied to each well. After that, each plate was incubated at 37 °C for a day. Each well zone of inhibition (measured in millimeters) was determined after incubation.

2.2.3.2. Antifungal activity

The disc diffusion method was used to examine the synthesized ZnO/ZrO₂/Al₂O₃ for its antifungal activities in vitro. In this study, Aspergillusflavus and Aspergillusniger were grown on potato dextrose agar (PDA). The normal

procedure was to make a well with a diameter of about 9 mm in the center of the agar medium, which had already been contaminated with fungus. The tested solutions (100 µL) were carefully put to the plate using a micropipette and it was then incubated at 37°C for three days. In the meantime, the infected fungi grew and the test solution did as well. Monitor the growth of the inhibitory zone on the plate. Fluconazole was used as a reference chemical for the study.

2.2.3.3. Minimum inhibitory concentration

The MIC test for the serial plate dilution procedure in DMSO is performed using the resulting ZnO/ZrO₂/Al₂O₃ screen. The nanocomposite and controls were serially diluted to logarithmic magnitudes in the nutrient broth, included c.f.u 104 mL-1 composing unit) of actively reproducing bacterial cells. Spectrophotometry and visual inspection were used to measure the magnification at 600 nm after the cultures were cultivated for 24 hours at 37 °C. The lowest concentration (maximum dilution) required to observe the bacterial multiplication is known as the minimum inhibitory concentration or MIC.

2.2.3.4. Antioxidant activity

With an odd electron, DPPH has an absorption peak at 517 nm. When the unpaired electrons in the DPPH moiety pair off, the absorbance decreases stoichiometrically with the number of electrons utilized. Determining how well various compounds can scavenge free radicals has been made much easier by this change in absorbance from the ensuing reaction. By providing the stable radical, DPPH was used to examine the compounds' capacity to scavenge free radicals in the hydrogen-donating or radicalscavenging capacity. To make the sample stock solutions (1 mg/mL), DMSO was used to dissolve the proper amount of DPPH. Up to 3 mL of methanol was added to stock solutions, causing concentration variations (0.2-1.0 \times 10-2 μ L). The DPPH solution was utilized for the previously tested solution. The absorbance at 517 nm was measured after the resulting mixture was well shaken and allowed to sit for 30 minutes. The results were presented as mean ± standard deviation (S.D.) with each estimate being carried out three times. Ascorbic acid served as the experiment's standard or positive and it was used as the negative control both with and without the test chemical or standard. The following formula was used to determine the DPPH radical scavenging ability:

 $I(\%) = (A_{blank} - A_{sample} / A_{blank}) \times 100$

Where A_{blank} is the absorbance of the control reaction mixture that contains the test compounds and A_{sample} is the absorbance of the test compounds.

3. Results and Discussion 3.1.X- ray Diffraction(XRD)

The produced $ZnO/ZrO_2/Al_2O_3$ nanocomposite XRD pattern, which shows distinct diffraction peaks, appears in Fig. 1a. The presence of ZnO is confirmed by the 2θ values of the peaks 31.95° , 34.42° , 36.32° , 47.68° , 56.56° ,

67.92° and 69.06° according to Treor programming (IUCR) which correspond to crystal planes of the (hkl) values (100), (002), (101), (102), (110), (112) and (201) respectively [JCPDF No. 36-1451]. The presence of ZrO₂ is confirmed by the 2θ values 30.07° , 41.43 and 62.81° which correspond to the crystal planes of the (hkl) values (-111), (111) and (-202) respectively [JCPDF No. The presence of Al_2O_3 01-083-0940]. confirmed by the 2θ values 38.01° and 76.82° , which correspond to crystal planes of the (hkl) values (110) and (119) accordingly [JCPDF No. 10-0173].

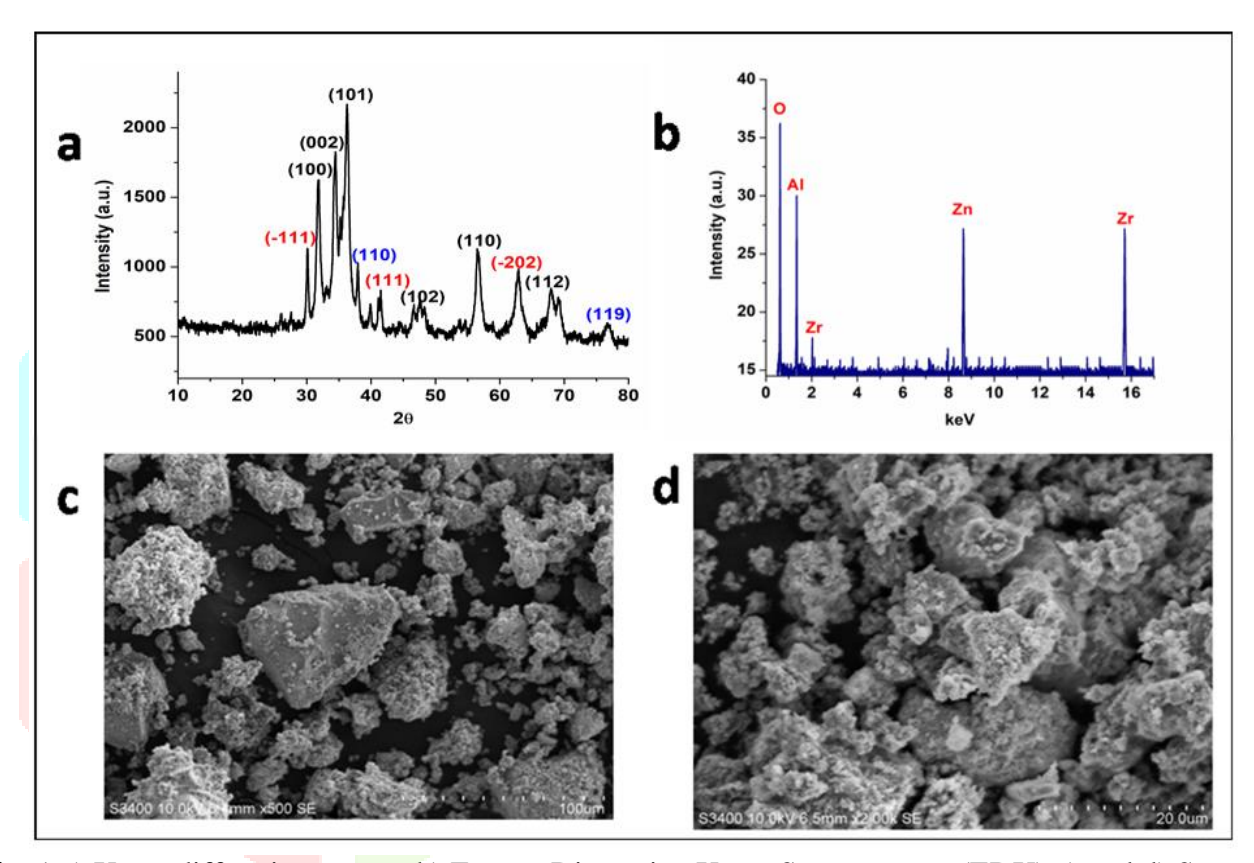


Fig. 1.a) X-ray diffraction pattern b) Energy Dispersive X-ray Spectroscopy (EDX) c) and d) Scanning Electron microscope images of ZnO/ZrO₂/Al₂O₃ nanocomposite

3.2. The Energy Dispersive X-ray Spectroscopy (EDX)

The presence and relative abundance of the elements in the examined sample are shown in the Fig. 1b of EDX spectrum. Aluminum (Al) and oxygen (O) exhibit the largest peaks according to the peak intensities seen, indicating that they are the most prevalent elements in the sample. With oxygen having the highest intensity and aluminum coming in second, there is likely a significant amount of aluminum oxide (AlO₃) present as the main constituent. The mild peaks for zirconium (Zr) and zinc (Zn) show that their concentrations are lower. Based on relative peak intensities, we can approximate elemental percentages even though EDX is largely a qualitative and semi-quantitative approach. In the inset of Fig. 1b, the

atomic mass percentages of O (48.1%), Al (17.6%), Zr (16.5%), and Zn (17.8%) suggest that a metal oxide ZnO/ZrO₂/Al₂O₃ nanocomposite may be formed. The peaks at 0.52 keV (O), 1.5 keV (Al), 7.5 keV (Zr), and 8 keV (Zn) verify their presence. ZnO, Al₂O₃, and ZrO₂ are among the oxides that could be produced due to the high oxygen level.

3.3.Scanning Electron microscope images (SEM)

A heterogeneous surface morphology with irregularly shaped particles of varied sizes is seen by the ZnO/ZrO₂/Al₂O₃ nanocomposite SEM Fig. 1c and 1d, suggesting a polydisperse dispersion. The presence of smaller nanoparticles surrounding larger angular particles indicates partial

agglomeration and a high surface area. The observed rough and porous texture is advantageous for increasing surface reactivity and is typical of metal oxide nanocomposites. The ZnO, ZrO₂ and Al₂O₃ phases combine to generate this morphology, which supports the composite's structural integrity and possible functional performance in coatings, sensors and catalysis, among other uses.

3.4.UV-Visible Spectroscopy

The graph supplied plots intensity (a.u.) wavelength (nm) to display versus ZnO/ZrO₂/Al₂O₃ nanocomposite's photoluminescence (PL) spectrum in Fig. 2a. A prominent emission peak at 380 nm is visible in the spectrum, which is indicative of nearultraviolet (UV) emission. This emission, which is usually ascribed to ZnO near-band-edge (NBE) recombination of electrons and holes, shows that ZnO is the composite main luminous component. The high intensity at this wavelength indicates that the nanocomposite has effective radiative recombination and good crystallinity. By altering defect states and improving structural stability, ZrO₂ and Al₂O₃ may affect emission intensity or deep-level emissions. Overall, the ZnO/ZrO₂/Al₂O₃ nanocomposite effective optical activity in the UV region is confirmed by the peak at 380 nm, which qualifies it for use in UV photodetectors, light-emitting devices and photocatalysis.

3.5.Band Gap Energy

The extrapolation of the linear region of the $(\alpha h \gamma)^2$ (eV)² (10⁻⁶) vs. (h γ) (eV) curve for the ZnO/ZrO₂/Al₂O₃ nanocomposite yield a Tauc plot that shows in a Fig. 2b direct optical band gap of roughly 3.2 eV. It is confirmed that the nanocomposite can absorb UV light because this band gap value is in line with ZnO optical characteristics. The material may be ideal for UV-based applications such as photocatalysis and optoelectronic devices due to the presence of ZrO₂

and Al₂O₃, which may improve the structural and thermal stability without substantially changing the band gap. This band gap value is typical for ZnO-based nanocomposites, indicating that the ZnO/ZrO₂/Al₂O₃ nanocomposite maintains the broad band gap characteristic of ZnO while the inclusion of ZrO₂ and Al₂O₃ may provide improved thermal or structural stability. The material's capability for UV light absorption is further confirmed by its 3.2 eV band gap, which makes it a promising candidate for use in photocatalysis, UV photodetectors or optoelectronic devices.

3.6.Percentage degradation of IC Dye

The Fig. 2c shows the Indigo Carmine dye photocatalytic degradation efficiency over time using various catalysts. With a degradation performance of almost 100% in just 10 minutes, the ZnO/ZrO₂/Al₂O₃ nanocomposite outperforms the other investigated materials, ZnO, ZrO₂ and Al₂O₃. High activity is also seen by ZnO alone, ZrO₂ and Al₂O₃. The synergistic impact of combining ZnO potent photocatalytic activity with the structural stability and surface area contributions of ZrO₂ and Al₂O₃ is responsible for the nanocomposite's improved degradation. This indicates the excellent effectiveness of the ZnO/ZrO₂/Al₂O₃ nanocomposite for quick and fast photocatalytic dye removal.

image The shows that the ZnO/ZrO₂/Al₂O₃ nanocomposite degrades the IC dye by over 100% in 5 minutes and keeps this high efficiency throughout time. Similar rapid degradation is seen in pure ZnO, which rapidly approaches 100%. On the other hand, after 5 minutes, ZrO₂ and Al_2O_3 exhibit deterioration levels, around 90–95% and 80–85%, respectively, and then stay comparatively stable. When compared to individual components, the nanocomposite exhibits better photocatalytic performance overall, particularly during the early phases of degradation.

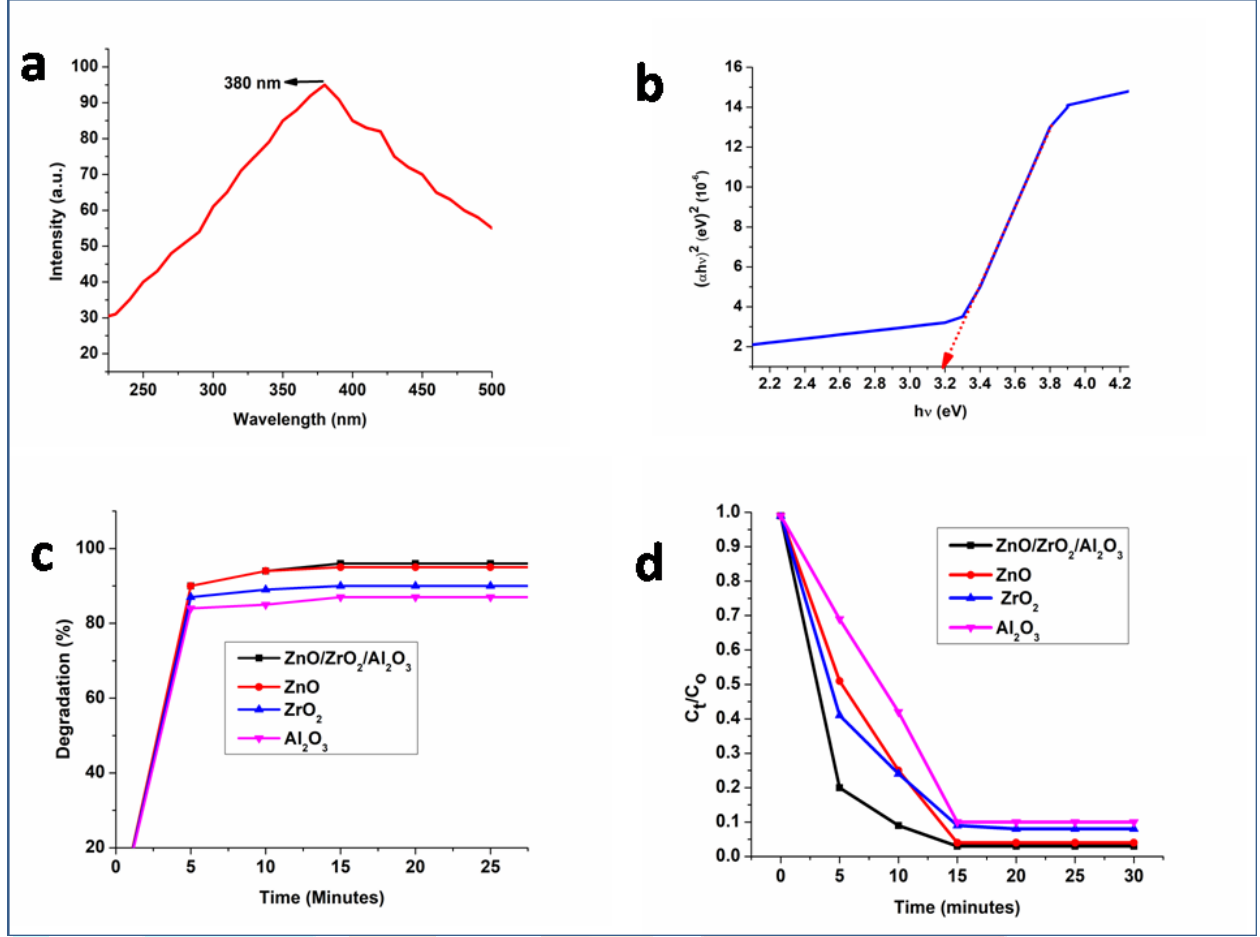


Fig. 2.a) UV-Visible Spectroscopy, b) Band Gap Energy c) Photocatalytic properties, d) Percentage degradation of IC Dye using ZnO/ZrO₂/Al₂O₃ nanocomposite

3.7.Photocatalytic Indigo Carmine Dye degradation

Through the gradual decline in concentration ratio (C_t/C_0) of IC dye, the Fig. 2d illustrates the photocatalytic characteristics of various materials. The nanocomposite ZnO/ZrO2/Al2O3 shows the fastest dve concentration drop, indicating greater photocatalytic activity. Pure ZnO comes in second. ZrO₂ and Al₂O₃ exhibit relatively slower rates of deterioration, with Al₂O₃ exhibiting the least effectiveness. Given their capacity to produce reactive species when exposed to light, which efficiently breaks down the dye molecules, the nanocomposite and ZnO appear to be very effective photocatalysts, as evidenced by the sharp drop that occurs within the first five minutes. All things considered, these findings demonstrate how nanocomposite photocatalytically than the separate oxides.

3.8.Effect of Catalytic concentration

Since the ZnO/ZrO₂/Al₂O₃ nanocomposite has more active sites and greater photocatalytic activity, it exhibits a strong catalytic effect on degradation efficiency that rises sharply with concentration up to about 0.3 g/L shows in the Fig. 3a. The metal oxides synergistic interaction, which enhances charge separation and light

absorption, is responsible for this. At greater concentrations (over 0.8 g/L), the efficiency plateaus and then slightly declines, most likely as a result of light scattering and particle aggregation. For efficient operation, the ideal catalyst concentration is therefore between 0.3 and 0.5 g/L.

3.9. Effect of dye concentration

The Fig. 3b indicates effective catalytic because ZnO/ZrO₂/Al₂O₃ activity the nanocomposite degradation efficiency is almost constant (~96%) at lower dye concentrations (10– 25 ppm). Nevertheless, the degradation efficiency progressively declines as the dye concentration rises above 25 ppm, reaching roughly 93% at 50 ppm. Since too much dye can block or absorb light and impede the photocatalytic process, this drop is probably caused by a lack of active sites and light penetration. Furthermore, intermediate products may build up as a result of increased dye concentrations, competing with dye molecules for active sites. Therefore, it is crucial to maintain a moderate dye concentration for the best degradation performance.

3.10. Effect of pH on IC Dye degradation

With the use of a ZnO/ZrO₂/Al₂O₃ nanocomposite, the Fig. 3c shows how pH affects the breakdown of indigo carmine (IC). With a high of almost 96%, degradation efficiency rises gradually from pH 4.0 to 6.9, suggesting increased catalytic activity in mildly acidic to neutral environments. Improved adsorption and photocatalytic reactions may result from the dye molecules and the nanocomposite ideal surface charge interactions at this pH. After pH 6.9, the degradation efficiency starts to decrease, most likely as a result of altered surface charge or stronger repulsion between the catalyst and dye at lower pH values. As a result, the ideal pH for this nanocomposite catalyst maximum degradation is 6.9.

3.11. Effect of Temperature on IC Dye degradation

The $ZnO/ZrO_2/Al_2O_3$ nanocomposite ability to degrade Indigo Carmine (IC) dye is highly dependent on temperature. The degradation efficiency often rises with temperature because of improved molecular mobility, which facilitates better interaction between the catalyst surface and dve molecules shows in Fig. 3d. Higher temperatures also speed up the production of reactive species like hydroxyl radicals, increasing the nanocomposite photocatalytic activity. This suggests that heat stimulation is beneficial to the endothermic breakdown process. Beyond an ideal temperature, however, the efficiency marginally decline because of increased recombination of photo-generated electron-hole pairs or potential catalyst particle agglomeration. Therefore, in order to achieve the highest degrading efficiency with the ZnO/ZrO₂/Al₂O₃ nanocomposite, it is essential to maintain a moderate temperature range.

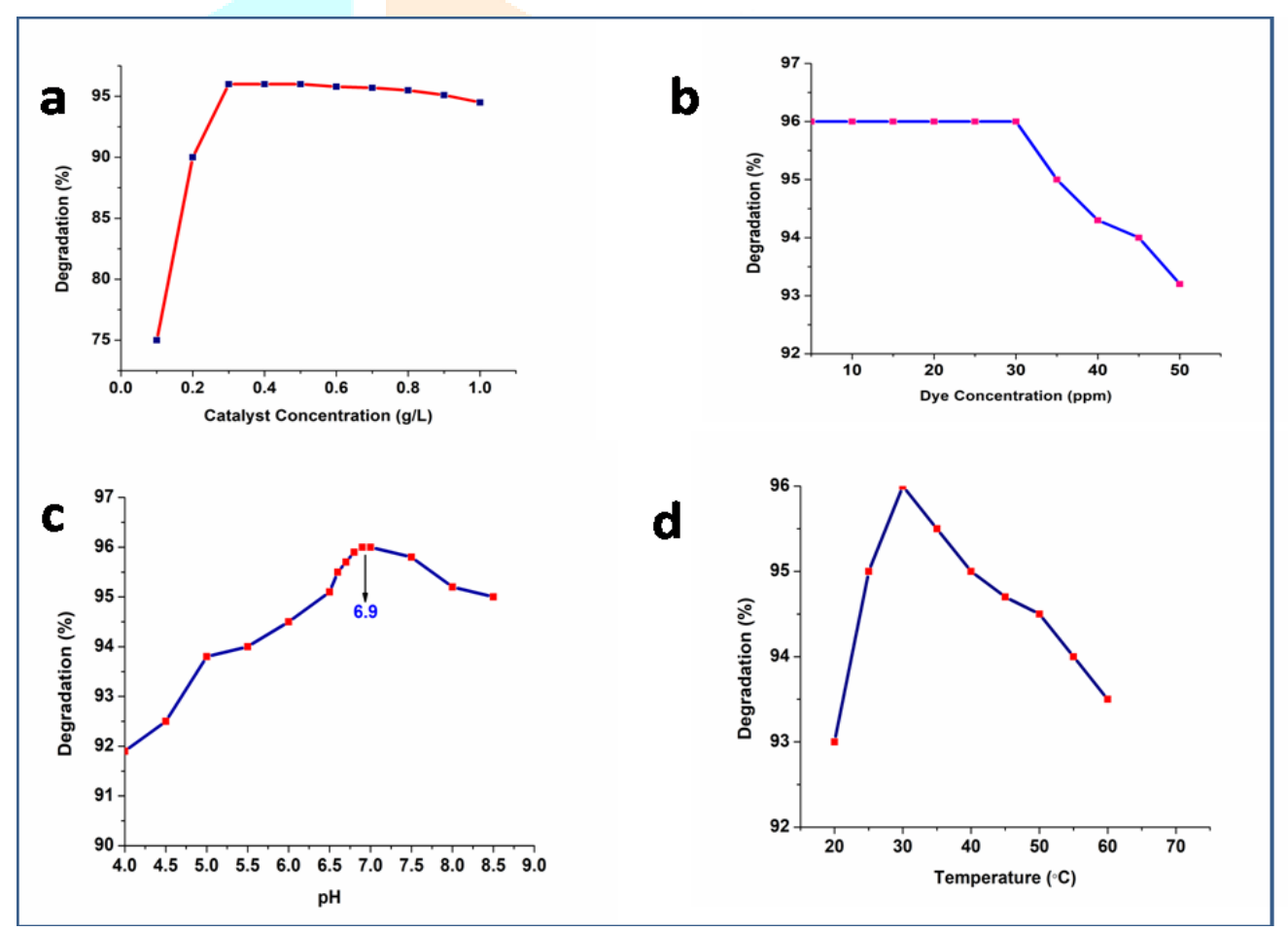


Fig. 3.a) Effect of Catalytic concentration, b) Effect of Dye concentration, c) Effect of pH, d) Effect of Temperature on IC dye degradation.

3.12. Mechanism of ZnO/ZrO₂/Al₂O₃ composite in photocatalytic degradation

The ZnO/ZrO₂/Al₂O₃ composite exhibits significant potential for visible-light-driven photocatalysis, particularly in the region of the solar spectrum ranging from approximately 400 to 800 nm. This is primarily attributed to the narrow band gap of ZnO (~3.37eV), which allows it to absorb photons in the ultra violet region effectively, while the presence of ZrO2 aids in charge separation and Al₂O₃contributes to structural stability and dispersion of active sites. Indigo Carmine (organic pollutant) is used to assess the photocatalytic activity of synthesized specimens upon exposure to visible light. For comparison, the photo catalytic activity of the pure ZnO, ZrO₂ and Al₂O₃ were also measured. Al₂O₃ alone show a very low photocatalytic activity.

During the experiment the UV light energy was absorbed by the ZnO nanoparticle, the energy able to excite electron from valence band of ZnO to conduction band of ZnO. Therefore electron (e⁻) moved to conduction band and hole (h⁺) present in valence band. Sometimes the formed hole (h⁺) and electron (e⁻) recombined, the degradation efficiency will be decreased due to unavailability of hole (h⁺) and electron (e⁻) for the photocatalysis. Therefore the presence of ZrO₂ helps to separate the hole and electron by interfacial charge separation р-р heterojunction between ZnO and ZrO₂. When the hole (h⁺) and electron (e⁻) get separated by ZrO₂ the photodegradation efficiency of the ZnO/ZrO₂/Al₂O₃ composite increase to 96%. The Al₂O₃ nanoparticle with large surface area was helpful for the better **dispersion** of ZnO and ZrO₂ nanoparticle, reduced agglomeration and acts as physical barrier by minimizing recombination effect.

The photogenerated (Excited) electrons from ZnO react with dissolved oxygen to form superoxide radicals. Meanwhile, photogenerated holes (now in ZrO₂) can oxidize water or hydroxide ions to form hydroxide radical. These radicals are highly reactive and non-selectively degrade organic dyes. The generated radicals attack the Indigo Carmine dye molecules, breaking down their chromophoric structures finally to form H₂O and CO₂.

3.13. Biological activity

3.13.1.Antimicrobial activity

In an invitro antibacterial experiment (Fig.4), the freshly created composite was evaluated against B. subtilis, L. monocytogenes, S. aureus, and P. aeruginosa. Additionally, two fungi, A. flavus and A. niger, were evaluated in order to determine the invitro antifungal activity. The prime range of the zone of inhibition was identified by physically inspecting the vicinity of each well. The zone of inhibition around each well was measured using the zone size in millimeters (mm). Table 1 summarizes and quantifies the inhibitors against both Grampositive and Gram-negative bacteria.

Table.1. Results of antiffictoblar activity of as synthesized ZhO/ZhO2/Ah2O3 hanocomposite								
Zone of inhibition (mm) ^a								
		Bacteria		Fungi				
Nano composite	L.	B.	S.	<i>P</i> .	A.	A.		
_	Monocytogenes	subtilis	aureus	aeruginosa	niger	flavus		
ZnO/ZrO ₂ /Al ₂ O ₃	10	9	13	11	12	9		
Ampicillin	23	24	25	27				
Fluconazole					20	22		

Table.1.Results of antimicrobial activity of as synthesized ZnO/ZrO₂/Al₂O₃ nanocomposite

The results obtained from the average of three replicates.

3.13.2. Minimum inhibitory concentration

By cultivating the bacterial cultures overnight, varying the concentration and applying the McFarland turbidity standard, the resultant nanocomposite minimum inhibitory concentration (MIC) was determined. The serial dilution approach was employed to ascertain the MIC of ZnO/ZrO₂/Al₂O₃ in the microtitre plate assay. The generated nanocomposite MIC range strongly inhibits both Gram positive and Gram negative microorganisms (Table 2). Because of the zinc, zerconium and allunium oxides composite, the resulting ZnO/ZrO₂/Al₂O₃ nanocomposite showed significant antibacterial activity. The Overtone concept of cell permeability illustrates that only soluble molecules are allowed to flow past the lipid membrane that encloses the cell. The outcomes clearly suggest that the produced nanocomposite can be used to treat bacteria that are resistant to treatment.



Fig. 4: The bactericidal activity of ZnO/ZrO₂/Al₂O₃ and control on *P. aeruginosa*

Table. 2. Minimum inhibitory concentration results

Range of concentration (µg/mL)								
	Bacteria			Fungi				
Nano composite		L.	B.	S.	Р.	A.	A.	
	Mono	cytogenes	subtilis	aureus	aeruginosa	niger	flavus	
ZnO/ZrO ₂ /Al ₂ O ₃		85	93	92	97	81	86	
Ampicillin		28	29	24	26			
Fluconazole				-4		48	46	

The results obtained from the average of three replicate analyses

3.13.3. Antioxidant activity

The DPPH assay was used to evaluate the nanocomposite ability to scavenge free radicals. The resulting nanocomposite capacity to act as an electron transfer in converting the DPPH radical from its radical state to the reduced form, DPPH-H, was investigated using the DPPH test. The ability of the nanocomposite to energetically scavenge the DPPH radical was evaluated in comparison to regular ascorbic acid. The

absorbance at 517 nm was used to measure its efficacy. The reaction mixture antioxidant activity was demonstrated by the color changing from deep purple (DPPH radical) to yellow (DPPH-H). The presence of free radical scavenge activity was indicated by the reaction mixture lowered absorbance value. The IC₅₀ value of the ZnO/ZrO₂/Al₂O₃ nanocomposite was comparable to that of ascorbic acid.

Table.3: Antioxidant ability (IC50) of all the synthesized compounds

Compounds	$IC_{50} (\mu g/mL) \pm S.D^*$		
AA	24±0.55		
ZnO/ZrO ₂ /Al ₂ O ₃	61±0.29		

AA = Ascorbic acid *S.D = Standard deviation (average of three replicates)

Summary and Conclusion

For usage in photocatalysis and bacterial inactivation, nanoscale ZnO/ZrO₂/Al₂O₃ has been created using a simple and eco-friendly electrochemical technique. When exposed to UV light, the generated nanocomposite showed outstanding photocatalytic activity in degrading the color indigo carmine. A higher catalytic efficiency was achieved using only 0.6g of catalyst. Both the overall degradation and catalytic

efficiency were evaluated using the chemical oxygen demand (COD) method. The antibacterial activity of the generated ZnO/ZrO₂/Al₂O₃ nanocomposite demonstrates its influence on biological systems.

A ZnO/ZrO₂/Al₂O₃ nanocomposite was successfully created in this study by an electrochemical process and its dual uses in photocatalytic dye degradation and antibacterial

activity were assessed. The successful creation of the composite with improved structural and optical qualities was validated by characterization. Because of the metal oxides synergistic interactions, increased surface area, and efficient charge carrier separation, the nanocomposite demonstrated a markedly improved photocatalytic degradation efficiency of indigo carmine (IC) dye under UV light. Furthermore, the production of reactive oxygen species, which damages

microbial cell membranes, was responsible for the high antibacterial activity seen against both Grampositive and Gram-negative bacteria. The ZnO/ZrO₂/Al₂O₃ nanocomposite is a highly promising material for environmental remediation applications, especially in wastewater treatment and microbial control, according to these findings. It provides an effective, environmentally friendly and multipurpose solution to pollution and public health issues.

Reference

- **1.** Adams FC, Barbante C. Nanoscience, nanotechnology and spectrometry. SpectrochimicaActa Part B: Atomic Spectroscopy. 2013 Aug 1;86:3-13.
- **2.** Avouris P. Manipulation of matter at the atomic and molecular levels. Accounts of chemical research. 1995 Mar 1;28(3):95-102.
- **3.** Thakur P, Thakur A. Introduction to nanotechnology. Synthesis and applications of nanoparticles. 2022 Jun 21:1-7.
- **4.** Gouadec G, Colomban P. Raman Spectroscopy of nanomaterials: How spectra relate to disorder, particle size and mechanical properties. Progress in crystal growth and characterization of materials. 2007 Mar 1;53(1):1-56.
- **5.** Asha AB, Narain R. Nanomaterials properties. In Polymer science and nanotechnology 2020 Jan 1 (pp. 343-359). Elsevier.
- **6.** Nasrollahzadeh M, Sajadi SM, Sajjadi M, Issaabadi Z. An introduction to nanotechnology. In Interface science and technology 2019 Jan 1 (Vol. 28, pp. 1-27). Elsevier.
- **7.** Sanjay SS, Pandey AC. A brief manifestation of nanotechnology. InEMR/ESR/EPR spectroscopy for characterization of nanomaterials 2016 Nov 10 (pp. 47-63). New Delhi: Springer India.
- **8.** Saleh TA. Nanomaterials: Classification, properties and environmental toxicities. Environmental Technology & Innovation. 2020 Nov 1;20:101067.
- 9. Ihde D. From Heideggerian industrial gigantism to nanoscale technologies. Foundations of Science. 2022 Mar 1:1-3.
- **10.** Roco M, Renn O, Jäger A. Nanotechnology risk governance. InGlobal risk governance: concept and practice using the IRGC framework 2008 Dec 18 (pp. 301-327). Dordrecht: Springer Netherlands.
- **11.** Nasrollahzadeh M, Sajadi SM, Sajjadi M, Issaabadi Z. An introduction to nanotechnology. InInterface science and technology 2019 Jan 1 (Vol. 28, pp. 1-27). Elsevier.
- **12.** Adams FC, Barbante C. Nanoscience, nanotechnology and spectrometry. SpectrochimicaActa Part B: Atomic Spectroscopy. 2013 Aug 1;86:3-13.
- 13. Omran BA. Nanobiotechnology: a multidisciplinary field of science. Cham: Springer; 2020 Aug 25.
- **14.** Thorkelsson K, Bai P, Xu T. Self-assembly and applications of anisotropic nanomaterials: A review. Nano Today. 2015 Feb 1;10(1):48-66.
- **15.** Calandra P, Caschera D, Liveri VT, Lombardo D. How self-assembly of amphiphilic molecules can generate complexity in the nanoscale. Colloids and Surfaces A: Physicochemical and Engineering Aspects. 2015 Nov 5;484:164-83.
- **16.** Fiedler B, Gojny FH, Wichmann MH, Nolte MC, Schulte K. Fundamental aspects of nanoreinforced composites. Composites science and technology. 2006 Dec 18;66(16):3115-25.
- **17.** Karger-Kocsis J, Mahmood H, Pegoretti A. All-carbon multi-scale and hierarchical fibers and related structural composites: A review. Composites Science and Technology. 2020 Jan 20;186:107932.
- **18.** Feng Y, Hao H, Lu H, Chow CL, Lau D. Exploring the development and applications of sustainable natural fiber composites: A review from a nanoscale perspective. Composites Part B: Engineering. 2024 Mar 8:111369.
- **19.** Oluwalowo A, Nguyen N, Zhang S, Park JG, Liang R. Electrical and thermal conductivity improvement of carbon nanotube and silver composites. Carbon. 2019 May 1;146:224-31.

- **20.** Cao R, Chen S, Wang Y, Han N, Liu H, Zhang X. Functionalized carbon nanotubes as phase change materials with enhanced thermal, electrical conductivity, light-to-thermal, and electro-to-thermal performances. Carbon. 2019 Aug 1;149:263-72.
- **21.** Rahimi-Ahar Z, Ahar LR. Thermal, optical, mechanical, dielectric, and electrical properties of nanocomposites. European Polymer Journal. 2024 Jul 25:113337.
- **22.** Vaia RA, Maguire JF. Polymer nanocomposites with prescribed morphology: going beyond nanoparticle-filled polymers. Chemistry of materials. 2007 May 29;19(11):2736-51.
- **23.** Wang S, Luo Z, Liang J, Hu J, Jiang N, He J, Li Q. Polymer nanocomposite dielectrics: understanding the matrix/particle interface. ACS nano. 2022 Sep 15;16(9):13612-56.
- **24.** Devaraju A, Sivasamy P. Comparative analysis of mechanical characteristics of sisal fibre composite with and without nano particles. Materials Today: Proceedings. 2018 Jan 1;5(6):14362-6.
- **25.** Li RL, Thrasher CJ, Hueckel T, Macfarlane RJ. Hierarchically Structured Nanocomposites via a "Systems Materials Science" Approach. Accounts of Materials Research. 2022 Nov 22;3(12):1248-59.
- **26.** Yu X, Marks TJ, Facchetti A. Metal oxides for optoelectronic applications. Nature materials. 2016 Apr;15(4):383-96.
- **27.** Selvi KT, Sagadevan S. Recent developments in optoelectronic and photonic applications of metal oxides. Metal Oxides for Optoelectronics and Optics-Based Medical Applications. 2022 Jan 1:33-57.
- **28.** Dey A. Semiconductor metal oxide gas sensors: A review. Materials science and Engineering: B. 2018 Mar 1;229:206-17.
- **29.** Kim HJ, Lee JH. Highly sensitive and selective gas sensors using p-type oxide semiconductors: Overview. Sensors and Actuators B: Chemical. 2014 Mar 1;192:607-27.
- **30.** Chavali MS, Nikolova MP. Metal oxide nanoparticles and their applications in nanotechnology. SN applied sciences. 2019 Jun;1(6):607.
- **31.** Annie Sujatha R, Manirahulan K, Ida Florence Sharon E, Arun Kumar C. Metal and Metal Oxide Enabled Sensors for Biomedical Applications. In Emerging Sustainable Nanomaterials for Biomedical Applications 2024 Aug 25 (pp. 187-222). Cham: Springer Nature Switzerland.
- **32.** Chavali MS, Nikolova MP. Metal oxide nanoparticles and their applications in nanotechnology. SN applied sciences. 2019 Jun;1(6):607.
- **33.** Wang M, Tan G, Zhang B, Wang Y, Bi Y, Yang Q, Liu Y, Liu T, Wang Z, Ren H, Lv L. Synergistic integration of energy storage catalysis: a multifunctional catalytic material for round-the-clock environmental cleaning. Applied Catalysis B: Environmental. 2023 Feb 1;321:122052.
- **34.** Raza S, Hayat A, Bashir T, Chen C, Shen L, Orooji Y, Lin H. Electrochemistry of 2D-materials for the remediation of environmental pollutants and alternative energy storage/conversion materials and devices, a comprehensive review. Sustainable Materials and Technologies. 2024 May 8:e00963.
- **35.** Aneke M, Wang M. Energy storage technologies and real life applications—A state of the art review. Applied Energy. 2016 Oct 1;179:350-77.
- **36.** Theerthagiri J, Karuppasamy K, Lee SJ, Shwetharani R, Kim HS, Pasha SK, Ashokkumar M, Choi MY. Fundamentals and comprehensive insights on pulsed laser synthesis of advanced materials for diverse photo-and electrocatalytic applications. Light: Science & Applications. 2022 Aug 10;11(1):250.
- **37.** Dharmalingam P, Palani G, Apsari R, Kannan K, Lakkaboyana SK, Venkateswarlu K, Kumar V, Ali Y. Synthesis of metal oxides/sulfides-based nanocomposites and their environmental applications: A review. Materials Today Sustainability. 2022 Dec 1;20:100232.
- **38.** Raza S, Hayat A, Bashir T, Chen C, Shen L, Orooji Y, Lin H. Electrochemistry of 2D-materials for the remediation of environmental pollutants and alternative energy storage/conversion materials and devices, a comprehensive review. Sustainable Materials and Technologies. 2024 May 8:e00963.
- **39.** Das S, Sen B, Debnath N. Recent trends in nanomaterials applications in environmental monitoring and remediation. Environmental Science and Pollution Research. 2015 Dec;22:18333-44.
- **40.** Karak N. Nanocomposites of epoxy and metal oxide nanoparticles. InSustainable Epoxy Thermosets and Nanocomposites 2021 (pp. 299-330). American Chemical Society.
- **41.** Dubourg G, Pavlović Z, Bajac B, Kukkar M, Finčur N, Novaković Z, Radović M. Advancement of metal oxide nanomaterials on agri-food fronts. Science of the total environment. 2024 Apr 4:172048.
- **42.** Al-Abadleh HA, Grassian VH. Oxide surfaces as environmental interfaces. Surface Science Reports. 2003 Dec 1;52(3-4):63-161.
- **43.** Wu W, Huang ZH, Lim TT. Recent development of mixed metal oxide anodes for electrochemical oxidation of organic pollutants in water. Applied Catalysis A: General. 2014 Jun 20;480:58-78.

44. J, Kumar A, Khan M, Lo IM. Critical review of photocatalytic disinfection of bacteria: from noble metals-and carbon nanomaterials-TiO2 composites to challenges of water characteristics and strategic solutions. Science of the Total Environment. 2021 Mar 1;758:143953.

